Engineering Geology

Rock mass statistical homogeneity investigation along a highway corridor in Vietnam

--Manuscript Draft--

Manuscript Number:	
Article Type:	Research Paper
Keywords:	Rock discontinuity orientation; Rock mass statistical homogeneity; polar equal area pole plots; linear correlation analysis; contingency table analysis
Corresponding Author:	Pinnaduwa Kulatilake University of Arizona Tucson, AZ United States
First Author:	Thanh Truong Phi
Order of Authors:	Thanh Truong Phi
	Pinnaduwa Kulatilake
	Mawuko Luke Yaw Ankah
	Desmond Talamwin Sunkpal
	Xiaokang Zhao
	Ha Viet Nguyen
	Tung Duc Van
Abstract:	This study clearly illustrates that at present no solid objective method is available in the engineering geology or rock mechanics literature to firmly demarcate between the statistical homogeneity and non-homogeneity of rock masses. The study shows that the available methods can only be used to rank rock masses with respect to the strength of statistical homogeneity. Three different methods, (a) polar equal area pole plot comparison, (b) linear correlation coefficient analysis and (c) contingency table analysis, are applied in this paper to evaluate the statistical homogeneity of rock masses that exist along a 15 km stretch of the 3B Highway corridor in Vietnam. The study clearly illustrates that application of different methodologies can lead to different ranking orders on the strength of statistical homogeneity of rock masses. That implies the difficulty in making a judgement on rock mass statistical homogeneity using results obtained from only one method. The paper shows how better decisions were made on rock mass statistical homogeneity by comparing the results obtained from the three different methodologies using only discontinuity orientation data.
Suggested Reviewers:	Wu Qiong China University of Geosciences wuqiong@cug.edu.cn
	Amitava Ghosh NRC, USA amitava.ghosh@sbcglobal.net
	Mousa Hazrati Aghchai Amirkabir University of Technology mousahazrati@aut.ac.ir
	Ove Stephansson GFZ: Deutsches Geoforschungszentrum Potsdam ove@gfz-potsdam.de

Rock mass statistical homogeneity investigation along a highway corridor in Vietnam

Thanh Truong Phi[a], Pinnaduwa H.S.W. Kulatilake[b,*], Mawuko Luke Yaw Ankah[b], Desmond Talamwin Sunkpal[b], Xiaokang Zhao[b], Ha Viet Nguyen[c], Tung Duc Van[d]

[a]*Hanoi University of Natural Resources and Environment, Vietnam*

[b]*School of Resources and Environmental Engineering, Jiangxi University of Science and Technology, Ganzhou, Jiangxi, 341000, P.R.China*

[c]*Hanoi University of Mining and Geology, Hanoi, Viet Nam*

[d]*Institute of geological Sciences, Viet Nam Academy of Science and Technology, Vietnam*

*Corresponding author: Pinnaduwa H.S.W. Kulatilake; E-mail address: kulatila@u.arizona.edu

Abstract

This study clearly illustrates that at present no solid objective method is available in the engineering geology or rock mechanics literature to firmly demarcate between the statistical homogeneity and non-homogeneity of rock masses. The study shows that the available methods can only be used to rank rock masses with respect to the strength of statistical homogeneity. Three different methods, (a) polar equal area pole plot comparison, (b) linear correlation coefficient analysis and (c) contingency table analysis, are applied in this paper to evaluate the statistical homogeneity of rock masses that exist along a 15 km stretch of the 3B Highway corridor in Vietnam. The study clearly illustrates that application of different methodologies can lead to different ranking orders on the strength of statistical homogeneity of rock masses. That implies the difficulty in making a judgement on rock mass statistical homogeneity using results obtained from only one method. The paper shows how better decisions were made on rock mass statistical homogeneity by comparing the results obtained from the three different methodologies using only discontinuity orientation data.

Keywords: Rock discontinuity orientation, Rock mass statistical homogeneity, polar equal area pole plots, linear correlation analysis, contingency table analysis.

Declarations

Funding/Acknowledgements

The first author would like to thank the Ministry of Natural Resources and Environment, Vietnam for providing financial support through the project Code: TNMT.2018.03.18 to work on the paper. The financial supports the second author received from the Jiangxi Province and the Chinese Government through the Distinguished Foreign Expert Talent Program Funding are gratefully acknowledged.

Conflict of interest/competing interest

The authors declare that they have no conflict of interest.

Availability of data and material

Possibility exists to make data available after publishing the papers in journals.

Code availability

Not applicable

1. Introduction and literature review

The mechanical and hydraulic behaviour of discontinuous rock masses as well as rock slope stability depend very much on the discontinuity geometry pattern of the rock masses (**Kulatilake et al. 1993 and 1996**). The discontinuity geometry pattern in a rock mass can vary from one region to another. The first step in determining the discontinuity geometry pattern in a rock mass is the identification of statistically homogeneous regions (**Kulatilake et al. 1993 and 1996**). It is also known as determination of structural domains in the traditional rock mechanics literature. Once the statistically homogeneous regions are determined, each one of these regions may be represented by a discontinuity geometry model. Such a discontinuity geometry model can then be used to study the mechanical or hydraulic behaviour or the rock slope stability of the rock mass. For complete statistical homogeneity of rock mass regions, the discontinuity sets should have similar distributions for discontinuity intensity in three dimensions, orientation, spacing, size, shape, roughness, and discontinuity constitutive properties. However, it is very difficult or almost impossible to achieve the statistical homogeneity to this level in rock engineering practice. At present, in practice, only the number of discontinuity sets and their orientation distributions are considered in determining the statistical homogeneity of rock masses. In practice, mostly, such rock masses are determined by visually comparing samples of geologic structure orientations, each of which consists of discontinuity normal vectors (also known as poles) plotted on a polar equal-area net. When discontinuity orientations do not show definite pole clusters, visual comparisons are often not sufficient to evaluate statistical homogeneity between chosen regions. Even when discontinuity orientations show definite pole clusters, in many cases it is difficult to compare the distribution of poles for a discontinuity set in the

considered two regions only through visual inspection. In such situations, it may be desirable to use the statistical procedures suggested by **Miller (1983), Mahtab and Yegulalp (1984), Kulatilake et al. (1990) and Martin and Tannant (2004),** and the fractal procedure suggested by **Kulatilake et al. (1997),** in addition to the visual examination of pole plots plotted on a polar equal-area net to investigate statistically homogeneous regions in rock masses. Attempts have been made to investigate statistical homogeneity of rock masses in a few sites in the world using discontinuity geometry data (**Kulatilake et al. 1990, 1996 and 1997; Martin and Tannant 2004; Phi et al. 2012; Thanh et al. 2015; Li et al. 2015; Song et al. 2018**). In these papers' authors had to make subjective decisions on statistical homogeneity of rock masses under significant uncertainty. The reason for that is the lack of a solid objective procedure in the current rock mechanics or engineering geology literature to firmly demarcate between the statistical homogeneity and non-homogeneity for real world rock masses. It is important to mention that decision making on statistical homogeneity for real world sites is a very difficult, challenging assignment. It is not a trivial task at all. It cannot be made in a firm, deterministic fashion. However, this aspect is not clearly shown through detailed case studies in the literature. One of the main aims of this paper is to show this difficult and challenging aspect through a very carefully performed detailed case study. Only joint orientation values are required to obtain pole plots on a polar equal area net, and to apply **Miller (1983), Kulatilake et al. (1990) and Martin and Tannant (2004)** procedures. On the other hand, discontinuity trace maps are required to apply the fractal procedure given by **Kulatilake et al. (1997)**. This paper first reviews the salient features and the capabilities of the polar equal area pole plots and **Miller (1983), Kulatilake et al. (1990) and Martin and Tannant (2004)** procedures. The paper then shows how modified versions of these procedures are applied to 4189 orientation data to investigate statistical homogeneity of rock masses located along a highway corridor in Vietnam. The obtained results very clearly show the difficult and challenging nature of decision making on statistical homogeneity of rock masses.

Fig. 1. Trajectories of the maximum compressive stress within the Indochina Peninsula during (a) the Oligocene and (b) at the present time (Kasatkin et al., 2014). The legend on the map in Figure 1 is described as follows: 1. trajectories of the maximum compressive stress: (a) which are directly related to the Indo-Eurasian plate collision and (b) its far-field effects; (2) faults and directions of displacement (arrows); (3) zone of continental collision; (4) subduction zone; (5) extension structures; (6) spreading zones; (7) current position of the land; Red River Fault System (RRFS); Cao Bang - Tien Yen fault (CB - TY).

2. Geological conditions of the considered site

The study area lies between two major fault zones (Red River fault zone and Cao Bang- Tien Yen fault zone) with the faults striking in the NW-SE direction in the Xuat Hoa area, Bac Kan Province (northeast region) of Vietnam (**Fig. 1**). Earlier studies (**Nguyen, 1991, Phung et al. 1996**) suggested that the study area has undergone two major phases of tectonic activity; an early phase compressive tectonic activity

occurred in the E-W direction starting from the Eocene and extending to the Oligocene-Miocene period followed by a late phase compressive tectonic activity in the N-S direction beginning from the Pliocene to the present (**Fig. 1**). Based on results of an extensive analysis of fault plane striations, **Thanh (2019)** identified four main compressive tectonic activity phases in the study area; the order and direction of occurrence of these phases are (a) NW-SE, (b) E-W, (c) NE-SW, and d) N-S. The geological map of the study area (**Nguyen et al. 2000**) along with the survey stations (SS) used to collect discontinuity orientation data are shown in **Fig. 2.** Note that the survey stations are selected along a highway named as the 3B Highway. As shown in **Fig. 2**, it is a highly winding road. It is very important to keep the rock slopes stable along this highway corridor. The rock mass statistical homogeneity of the highway corridor is investigated in this paper as the first step towards investigating rock slope stability. As explained above, the tectonic condition of the study area is quite complex. Therefore, intuitively, a quite complex rock mass statistical homogeneity can be expected along the highway corridor. The dominant lithologies in the study area are Devonian sedimentary rocks. These rocks belong to three main formations as shown in **Fig. 2**: a) Tam Hoa formation ($D_{2\text{-}3}th$) consisting of polymictic conglomerate, gritstone, clayey shale and limestone; b) Mia Le Formation (D_1ml_1 and D_1ml2) consisting of clayish siltstone and marlaceous shale; and c) Na Quan formation ($D_{1\text{-}2}nq_1$ and $D_{1\text{-}2}nq_2$) consisting of marlaceous shale and shale interbedded with limestone respectively. Typical rock masses of each of these formations located at a few survey stations are shown in **Fig. 3**.

Fig. 2. Geological map of the study area showing the survey stations (SS) used to obtain orientation data.

Fig. 3. Typical rock masses that exist at a few survey stations.

Discontinuity orientation data were collected from three formations at 32 survey stations located along a 15 km stretch of the 3B Highway corridor. The location map of the survey stations and the lithologies of the stations are shown in **Fig. 2**. The survey station SS-1, SS-4 through SS-11, and SS-13 through SS-32 are from the D_1ml_2 formation. The survey station SS-2 is from the D_1ml_1 formation. The survey station SS-3 is located at the boundary between the $D_{2\text{-}3}th$ and $D_{1\text{-}2}nq_2$ formations. The survey station SS-12 is from the $D_{1\text{-}2}nq_2$ formation. The survey stations SS-12 and SS-13 are on the opposite sides of a fault line. A very good chance exists to have poor statistical homogeneity when rock masses from opposite sides of a fault line are compared. If the formations are quite different, then there is a tendency to have a low level of statistical homogeneity among the rock masses located in different formations. A total of 4189 discontinuity orientation data were collected from the 3B Highway corridor as given in **Table 1**. A few details about each

survey station and the number of discontinuity orientation data collected from each station are presented in **Table 1**.

Table 1 Survey station locations, geologic age and the number of discontinuity orientation data collected for the various stations.

3. Main features of the procedures used to evaluate statistical homogeneity

3.1. Polar equal area pole plot comparison

Polar equal area net is used to plot the discontinuity normal vectors (also known as poles) of orientation data and to find the distribution of discontinuity poles for each discontinuity set belonging to a particular rock mass site (**Goodman 1976; Hoek and Bray 2004**). The pole plotting can be done either using the lower hemispherical projection or the upper hemispherical projection (**Goodman 1976**). In this study the lower hemispherical projection was used in plotting the discontinuity poles. These plots show pole concentrations. These pole concentrations can be used to determine the number of discontinuity sets that exists in a rock mass site. In addition, these pole plots show the distribution of orientation data for each discontinuity set. The polar equal area pole plots of two rock mass sites can be compared visually to assess the statistical similarity of the two sites based on the number of discontinuity sets that exists in the two sites and their orientation distributions. This statistical similarity is also worded as the rock mass statistical homogeneity of the two sites in this paper.

In determining the rock mass statistical homogeneity between two sites, efforts were made to draw visual conclusions about the strength of statistical homogeneity of two adjacent regions. This was achieved by using only the polar equal area pole plots to assign qualitative ranks of the rock mass statistical homogeneity. In investigating the statistical homogeneity between two rock mass sites, it is necessary to first check whether the same number of discontinuity sets appear in the two sites. If so, then it is necessary to check for each of the discontinuity sets, orientation wise, whether the same discontinuity set appears in the two data sites being compared. If the same discontinuity sets exist in the data sites, a further check on the similarity of their orientation distributions is conducted.

Generally, data sites which are in proximity in the same rock formation or similar rock formations tend to have stronger statistical homogeneity compared to sites that are far apart in the same rock formation or in different rock formations. First, the polar equal-area pole plots were compared among every two adjacent stations along the highway corridor starting from SS-1 versus SS-2 to SS-31 versus SS-32. If any two adjacent stations were found to be strongly statistically homogeneous, then the orientation data of those two stations were combined to make a new polar equal area pole plot for each of the combined stations.

Then the polar equal area pole plot of each of the combined stations was compared with the next adjacent station to evaluate the statistical homogeneity among those stations. This process was continued for all the adjacent stations along the highway corridor, which showed strong statistical homogeneity.

3.2. Linear correlation coefficient analysis

It is often difficult to evaluate the statistical homogeneity only by visually comparing the polar equal area plots of different sites when definite pole clusters do not appear through the discontinuity orientation data. Even when the pole clusters are visible, the qualitative nature of the polar equal area pole plot comparison procedure makes the result subjective. Such difficulties can be avoided by adopting quantitative methods such as the linear correlation coefficient, ρ, analysis and/or contingency table analysis in identifying statistically homogeneous domains. This section covers the linear correlation coefficient analysis. Section 3.3 covers the contingency table analysis. A polar equal area patch network was constructed by dividing the horizontal circumferential 0 to 360 degrees into 10-degree cells and horizontal radial 0 to 90 degrees on the polar equal area net into 10-degree cells. This created a 324-patch polar equal area net as shown in **Fig. 4.**

Fig. 4. The constructed 324-patch polar equal area net.

Poles of the discontinuity orientation data of each of the 32 stations were plotted using the lower hemispherical projection on the 324-patch polar equal area net. For each of the two station combinations considered under polar equal area plot comparison method (see section 3.1), the linear correlation coefficient, R (x, y), was calculated according to equation (1). The numerator of Eq. (1) is the covariance. The two square root terms appearing in the denominator of Eq. (1) are the standard deviations of x and y.

$$R(x,y)=\frac{\frac{1}{(n-1)}\sum_{i=1}^{n}(x_i-\bar{X})(y_i-\bar{Y})}{\sqrt{\frac{1}{(n-1)}\sum_{i=1}^{n}(x_i-\bar{X})^2}\sqrt{\frac{1}{(n-1)}\sum_{i=1}^{n}(y_i-\bar{Y})^2}} \quad (1)$$

In Eq. (1), $(x_1, y_1), (x_2, y_2), \ldots, (x_n, y_n)$ are n pairs of pole number observations coming from n 10 by 10 degree cells for each of the considered two stations. $\bar{X}$ and $\bar{Y}$ are the average pole numbers for a 10 by10-degree cell from each of the two stations considered in the computation. x_i is the pole number that appears in cell i of the first station and y_i is the pole number that appears in cell i of the second station. Because a 324-patch polar equal area net is used for the calculations, n = 324 for the conducted study. The sorting of discontinuity poles was done in such a way that no single discontinuity pole falls into two cells in a polar equal area net, which will result in double counting. R expresses the strength of the similarity or statistical

198 homogeneity of the pole distributions among the considered two stations. R values range from -1 to +1 and
199 do not depend on the discontinuity data numbers of the considered two stations. The R value of +1 implies
200 perfect positive linear correlation while the R value of -1 implies perfect negative linear correlation. The R
201 value of 0 implies no correlation. Low R values imply weak linear correlation and high R values imply
202 strong linear correlation. Higher the magnitude of the R, better the linear correlation and better the chance
203 for the statistical homogeneity. Unfortunately, it is not possible to specify an objective R value which
204 demarcates between the statistical homogeneity and non-homogeneity. Therefore, in this paper, the
205 computed R value is used to assign a rank to the tested two regions to indicate the strength of the rock mass
206 statistical homogeneity.
207
208 *3.3. Contingency table analysis*
209 Application of contingency table analysis to polar equal area plots requires the division of the lower
210 hemisphere into patches that have equal areas either on the lower or upper hemisphere. In this paper, the
211 lower hemisphere is chosen. In this study, a modified version of **Miller's method (1983)** reported by
212 **Kulatilake et al. (1990)** was used to perform contingency table analysis. Based on the modified Miller's
213 method, a formulation is given to divide the lower hemisphere polar equal area net into equal surface area
214 patches after selecting the number of dip bands and the number of patches (cells) in each band. Most of the
215 discontinuities of the survey stations were found to be of sub-verticals giving high dip angles. Therefore,
216 most of the poles were expected to get plotted in the polar equal area net within 0-40 degrees from the
217 periphery towards the center of the patch network. That means it is better to have 4 bands rather than 3,
218 which is usually used, for the patch network and more patches or cells in the outer two bands for better
219 discrimination of pole sorting to perform contingency table analysis. Based on these concepts, for the first
220 time a 68-cell patch network as shown in **Fig. 5** was designed to perform contingency table analysis.
221
222 **Fig. 5.** The designed 68-cell patch network used for the contingency table analysis.
223
224 **Table 2** Contingency table for analyzing the polar equal area plots of different stations (**after Miller, 1983**).
225
226 **Table 2** provides a contingency table for analyzing the polar equal area plots of different stations. Entry
227 of each patch (cell) in the table is the number of discontinuity poles that occur in that patch (f_{ij}). To test the
228 null hypothesis that the rock mass stations are statistically homogeneous, the following chi-square statistic
229 is calculated to perform the chi-square test.

$$\chi^2 = \sum_{i=1}^{r}\sum_{j=1}^{r}\frac{\left(f_{ij}-e_{ij}\right)}{e_{ij}} \quad (2)$$

In Eq. (2), e_{ij} is the expected number of discontinuity poles in the *ij* cell and it is calculated through $e_{ij} = (R_iC_j)/N$ (**Miller 1983; Kulatilake et al. 1990**). The symbols R_i and C_j are explained in **Table 2**. Under the null hypothesis, to have a perfect fit, all f_{ij} should be equal to e_{ij}. In such a case $\chi^2 = 0$. Thus, large values of χ^2 tend to discredit the null hypothesis, and small values of χ^2 tend to confirm the hypothesis. If the null hypothesis is true, then in general the calculated χ^2 is chi-square distributed with (r-1) (c-1) degrees of freedom. According to the usual chi-square test procedure, the null hypothesis is rejected if the χ^2 from Eq. (2) exceeds the value from the chi-square table corresponding to (r-1) (c-1) degrees of freedom at the chosen significance level of α. In statistical applications, the statisticians commonly use 0.05 or 0.10 for α. Another possibility is to obtain the α value from the chi-square table corresponding to the calculated χ^2 value from Eq. (2) using the degrees of freedom (r-1) (c-1). This value, termed as *p*, can be considered as one's confidence in accepting the null hypothesis and seems more appropriate to use in engineering applications.

The accuracy of the chi-square test depends on the e_{ij} distribution in the patch network. Miller recommends use of Lancaster's (**Lancaster, 1969**) criterion for contingency table analyses of equal area plots. To satisfy Lancaster's criterion, it will be necessary to try out different patch networks. It is possible to find equal area plots for which Lancaster's criterion cannot be met. For such situations, *p* can be evaluated using the approximation that χ^2 follows a normal distribution under the condition of degrees of freedom greater than 30.

The value obtained for *p* depends on the following factors: (a) the number of patches in the patch network; (b) the relative position of the patch network with respect to north; and (c) whether the Lancaster's criterion was met or not. Therefore, for the same data, it is possible to get several different values for *p*. Then one faces the almost impossible task of deciding on a value for *p* which demarcates between the statistical homogeneity and non-homogeneity. Therefore, it is not possible to determine rock mass statistical homogeneity uniquely through this method too as in the previous two methods. However, if the afore-mentioned three factors are kept the same in testing different regions of the rock mass, then the obtained *p* values can be used to rank the tested regions with respect to the strength of homogeneity. The chance for statistical homogeneity increases with increasing *p*. In this paper, 18 contingency test results are obtained for each tested two regions starting from the patch network aligned to north and then by rotating the patch network using an increment of 10 degrees. For each of these test results χ^2 and *p* values are obtained based

on both the chi-square and normal distributions. These 18 sets of values were then used to compute average χ^2 and average p values based on both the chi-square and normal distributions. These average p values are then used to rank each of the tested two regions with respect to the strength of statistical homogeneity.

4. Results

4.1. Use of polar equal area pole plot comparison to assign qualitative ranks of statistical homogeneity

Discontinuity orientation data collected from the 32 survey stations were plotted on the equal area polar net using the Dips 7.0 software package (**Rocscience Inc., 2019**) and selecting the lower hemisphere projection. The obtained lower hemispherical polar equal area pole plots are shown in **Fig. 6**. These plots show about two sub-vertical discontinuity sets. In certain stations both sets appear prominent. In the remaining stations only one prominent discontinuity set appears. For most of the stations, the orientation distributions and mean orientation directions of these two discontinuity sets vary from one station to another significantly. That weakens the strength of the statistical homogeneity among many stations. By looking at the polar equal area pole plots it is difficult to firmly demarcate between the statistical homogeneity and non-homogeneity between different stations. Therefore, an attempt was made to qualitatively rank the stations with respect to the strength of statistical homogeneity.

Fig. 6. Lower hemispherical polar equal area pole plots of the 32 stations located along the highway corridor.

The polar equal area pole concentration plots shown in **Fig. 6** were used in making a judgement about the strength of statistical homogeneity for each of the two adjacent stations located along the highway corridor. For each case, a qualitative rank was assigned based on the procedure mentioned under section 3.1. Poor (P), Low (L), low to poor (L-P), medium (M), or high (H) ranks were assigned to the cases to indicate the observed visual strength of statistical homogeneity. Note that this ranking procedure is subjective. The obtained results are given in **Table 3**. The stations SS-12 and SS-13 showed a very poor level of statistical homogeneity. Note that these two stations are located on the opposite sides of a fault. This result was intuitively expected. Rock formation differences among the tested two stations exist for the following cases: SS-1 versus SS-2, SS-2 versus SS-3, SS-3 versus SS-4 and SS-11 and SS-12. Note that all those cases show either a P, L-P or L level of statistical homogeneity. Possibility of a such a result was stated in section 3.1.

Table 3 Summary results for strength of statistical homogeneity based on different methods.

The obtained results from the polar equal-area pole plot comparisons of the discontinuity data **(Table 3**) indicate that the stations SS-20 versus SS-21, SS-26 versus SS-27, SS-27 versus SS-28 and SS-31 versus SS-32 have H level of statistical homogeneity among all the cases tested. These cases show existence of similar discontinuity sets with quite similar orientation distributions. The following cases showed M level statistical homogeneity based on existence of similar discontinuity sets and fairly similar orientation distributions: SS-5 versus SS-6, SS-10 versus SS-11, SS-14 versus SS-15, SS-15 versus SS-16, SS-18 versus SS-19, SS-19 versus SS-20, SS-28 versus SS-29 and SS-30 versus SS-31. Orientation data of locations that indicated existence of either H level or M level statistical homogeneity between adjacent stations were then combined as follows to make comparisons among equal area pole plots of combined stations: (a) SS-14 & 15 versus SS-16, (b) SS-18 versus SS-19 & 20, (c) SS-18 & 19 versus SS-20 & 21, (d) SS-26 & 27 versus SS-28, (e) SS-26 & 27 versus SS-28 & 29 and (f) SS-30 versus SS-31 & 32. Lower hemispherical polar equal area pole plot comparisons made for the combined stations are shown in **Fig. 7**. The qualitative rankings made through visual comparison are given in **Table 3**. These rankings were assigned based on the rankings made earlier using P through H levels. Out of all the stations compared, the stations 18 through 21 seem to indicate the highest level of statistical homogeneity.

Fig. 7. Lower hemispherical polar equal area pole plot comparisons made for the combined stations: (a) SS-14 & 15 versus SS-16 (L level), (b) SS-18 versus SS-19 & 20 (H level), (c) SS-18 & 19 versus SS-20 & 21 (M level), (d) SS-26 & 27 versus SS-28 (L level), (e) SS-26 & 27 versus SS-28 & 29 (L level) and (f) SS-30 versus SS-31 & 32 (L level).

4.2. Use of linear correlation coefficient analysis to assign quantitative ranks of statistical homogeneity

Using the procedure explained in section 3.2, the linear correlation coefficient, R, values were calculated for the same station cases mentioned under section 3.1. The obtained R values are given in **Table 3**. Based on these R values, ranks were assigned to indicate the strength of statistical homogeneity for the tested cases. Lower the rank number, the higher the strength of statistical homogeneity. Among every two stations tested, SS-20 versus SS-21, SS-26 versus SS-27 and SS-31 versus SS-32 produced the highest R values (0.50-0.58) indicating highest chance of statistical homogeneity. SS-5 versus SS-6, SS-10 versus SS-11, SS-14 versus SS-15, SS-15 versus SS-16, SS-18 versus SS-19, SS-19 versus SS-20, SS-25 versus SS-26, SS-27 versus SS-28, SS-28 versus SS-29 and SS-30 versus SS-31 produced moderate R values (0.32-0.48) indicating moderate chance of statistical homogeneity. SS-2 versus SS-3, SS-3 versus SS-4, SS-4 versus SS-5, SS-6 versus SS-7, SS-9 versus SS-10, SS-11 versus SS12, SS-16 versus SS-17, SS-22 versus SS23, and SS-24 versus SS-25 produced low R values (0.20-0.25) indicating low chance of statistical homogeneity. SS-1 versus SS-2, SS-7 versus SS-8, SS-8 versus SS-9, SS-12 versus SS-13, SS-13 versus

SS-14, SS-17 versus SS-18 and SS-21 versus SS-22 gave the lowest R values (less than 0.20) indicating poor chance of statical homogeneity. Note that the selection of demarcation boundaries for high, moderate, low, and poor was done subjectively based on the orientation distributions observed on the 324-patch network and the magnitude of R value. **Fig. 8** shows the pole plot comparisons obtained on the 324-patch network for the cases of SS-7 versus SS-8, SS-2 versus SS-3, SS-5 versus SS-6 and SS-26 versus SS-27 on R analysis as typical examples for poor, low, moderate, and high R values, respectively. Rankings seem to agree very well with the visual orientation distributions seen on 324-patch networks.

Fig. 8. Pole plot comparisons on the 324-patch network for R analysis as typical examples for poor, low, moderate, and high R values: (a) SS-7 versus SS-8 (poor R = -0.04), (b) SS-2 versus SS-3 (low R = 0.24), (c) SS-5 versus SS-6 (moderate R = 0.38) and (d) SS-26 versus SS-27 (high R = 0.58).

Orientation data of locations that indicated existence of either high or moderate R values among adjacent stations were then combined as follows to calculate R values for the combined stations: (a) SS-14 & 15 versus SS-16, (b) SS-18 versus SS-19 & 20, (c) SS-18 & 19 versus SS-20 & 21, (d) SS-26 & 27 versus SS-28, (e) SS-26 & 27 versus SS-28 & 29 and (f) SS-30 versus SS-31 & 32. The obtained R values are given in **Table 3**. Based on these R values, rankings were assigned based on the rankings 1-31 made earlier using the first 32 cases tested. If two numbers are used for the ranking, it means that the ranking is in-between the two numbers. SS-18 versus SS-19 and 20, and SS-18 and SS-19 versus SS-20 and SS-21 produced the same R value of 0.57, which is higher than that obtained for SS-18 versus SS-19 (R = 0.37), SS-19 versus SS-20 (R = 0.45) and SS-20 versus SS-21 (R = 0.50). R values obtained for SS-26 versus SS-27, SS-27 versus SS-28 and SS-28 versus SS-29 were 0.58, 0.48 and 0.35, respectively. R values obtained for SS-26 and SS-27 versus SS-28, and SS-26 and SS-27 versus SS-28 and SS-29 were 0.50 and 0.55, respectively. That means for these cases, the combined stations have produced R values which are in-between the R values obtained for the uncombined cases. SS-14 and SS- 15 versus SS-16 produced a R value of 0.30, which is lower than that obtained for the uncombined stations SS-14 versus SS-15 (R = 0.41) and SS-15 versus SS-16 (R = 0.33). SS-30 versus SS-31 and SS-32 produced a R value of 0.38, which is lower than that obtained for the uncombined stations SS-30 versus SS-31 (R = 0.43) and SS-31 versus SS-32 (R = 0.56). The afore-mentioned examples show that different scenarios are possible by combining the orientation data of adjacent stations. Out of all the combined stations compared, the stations SS-18 through SS- 21 seem to indicate the highest level of statistical homogeneity. Stations SS-26 through SS-29 indicate high level of statistical homogeneity. Stations SS-14 through SS-16 and SS-30 through SS-32 show moderate level of statistical homogeneity.

362 *4.3. Use of contingency table analysis to assign quantitative ranks of statistical homogeneity*

363 Using the procedure explained in section 3.3, the average *p* values were calculated for the same station
364 cases mentioned under section 3.1. The obtained average *p* values are given in **Table 3**. Based on these
365 average *p* values, ranks were assigned to indicate the strength of statistical homogeneity. Lower the rank
366 number, the higher the strength of statistical homogeneity. Among every two sites tested, SS-26 versus SS-
367 27, SS-20 versus SS-21, SS-10 versus SS-11 and SS-19 versus SS-20 produced the highest average *p* values
368 (0.37-0.66) indicating high chance of statistical homogeneity. SS-27 versus SS-28, SS-31 versus SS-32,
369 SS-5 versus SS-6, SS-30 versus SS-31, SS-16 versus SS-17, SS-14 versus SS 15, SS-15 versus SS-16 and
370 SS-18 versus SS-19 produced moderate average *p* values (0.16-0.33) indicating moderate chance of
371 statistical homogeneity. SS-22 versus SS-23, SS-4 versus SS-5, SS-28-versus SS-29, SS-11 versus SS-12
372 and SS-6 versus SS-7 produced low average *p* values (0.05-0.16) indicating low chance of statistical
373 homogeneity. The rest of every two stations tested gave the lowest average *p* values (0-0.05) indicating
374 poor chance of statistical homogeneity. Note that the demarcation boundary between poor and low
375 statistical homogeneity was selected based on the minimum significance level statisticians use for
376 acceptance of the null hypothesis of statistical homogeneity. Demarcation boundaries between low and
377 moderate, and moderate and high were selected subjectively based on the obtained average *p* values and
378 the visual observation of orientation distributions on the 68-patch network.
379
380 Orientation data of locations that indicated existence of either high or moderate average *p* values among
381 adjacent stations were then combined as follows to calculate average *p* values for the combined stations:
382 (a) SS-14 & 15 versus SS-16, (b) SS-18 versus SS-19 & SS-20, (c) SS-18 & SS-19 versus SS-20 & SS-21,
383 (d) SS-26 & SS-27 versus SS-28, (e) SS-26 & 27 versus SS-28 & SS-29 and (f) SS-30 versus SS-31 & SS-
384 32. The obtained *p* values are given in **Table 3**. Based on these average *p* values, rankings were assigned
385 based on the rankings 1-31 made earlier using the first 32 cases tested. If two numbers are used for the
386 ranking, it means that the ranking is in-between the two numbers. SS-18 versus SS-19 and SS-20 produced
387 a *p* value of 0.45, which is higher than that obtained for SS-18 versus SS-19 ($p = 0.16$) and SS-19 versus
388 SS-20 ($p = 0.38$). For this case, the statistical homogeneity has increased by combining the data of adjacent
389 stations. On the other hand, for all other combined station cases the obtained average *p* values were
390 significantly less than that obtained for the corresponding uncombined two station cases (see **Table 3**). This
391 indicates that the statistical homogeneity has decreased for these cases by combining the data from adjacent
392 stations. Based on the contingency table analysis results, out of all the combined stations compared, the
393 stations SS-18 through SS- 20 seem to indicate high level of statistical homogeneity. Stations SS-14 through
394 SS-16 indicate low level of statistical homogeneity. SS-26 through SS-29 and SS-30 through SS-32 show
395 poor level of statistical homogeneity. Note that the low and poor level statistical homogeneity results

obtained for the combined stations through contingency table analysis results are very different to the results obtained through R calculations. This is currently a puzzle. Note that the number of data increases when we combine the stations. The afore-mentioned discrepancy between the R calculation results and contingency analysis results might have resulted from increase of discrimination power of the contingency table analysis procedure with the increase of the number of data of the tested cases.

5. Conclusions

As shown in this paper, no solid objective method is available at present in the engineering geology or rock mechanics literature to firmly demarcate between the statistical homogeneity and non-homogeneity of rock masses. Each of the available methods can only be used to rank rock masses with respect to the strength of statistical homogeneity. Three different methods, (a) polar equal area pole plot comparison, (b) linear correlation coefficient analysis and (c) contingency table analysis, were applied in this paper to evaluate the statistical homogeneity of rock masses that exist along a highway corridor in Vietnam. The quantitative ranks obtained from the linear correlation analysis and the contingency table analysis have some similarities as well as some differences (see **Table 3**). Analysis performed for every two sites have provided quantitative rankings within 5 for 21 out of 31 tested cases, which is a significant similarity. For 2 out of 31 cases, the ranking difference is more than 12, which is a major difference. For 8 out of 32 cases, the ranking difference is between 6 and 8, which is a significant difference. For the calculations conducted on the combined stations through the two quantitative methods, only one case out of six has given a similar result; the rest of the five cases show drastic differences. Comparison of the results from the two quantitative methods clearly show that SS-26 versus SS-27 and SS-20 versus SS-21 indicate high chance of rock mass statistical homogeneity; SS-10 versus SS-11, SS-19 versus SS-20, SS-27 versus SS-28 and SS-31 versus SS-32 indicate medium to high statistical homogeneity. Comparison of the results from the two quantitative methods for SS-5 versus SS-6, SS-30 versus SS-31, SS-14 versus SS-15, SS-15 versus SS-16, SS-18 versus SS-19, SS-28 versus SS-29 and SS-16 versus SS-17 indicate medium level of rock mass statistical homogeneity. The compared results from the two quantitative methods for SS-22 versus SS-23, SS-4 versus SS-5, SS-11 versus SS-12 and SS-6 versus SS-7 show low level of rock mass statistical homogeneity. Comparison of the results from the two quantitative methods for the rest of the cases show poor level of statistical homogeneity. According to the quantitative ranking results, SS-26 versus SS-27 can be declared as the stations that show the highest chance of rock mass statistical homogeneity; SS-7 versus SS-8 can be declared as the stations that show the poorest chance of rock mass statistical homogeneity. For majority of the cases, the conclusions obtained through comparison of the rankings obtained from the two quantitative methods seem to agree reasonably well with the subjective qualitative rankings obtained through visual comparison of polar equal area pole plots of the orientation data. The study clearly illustrates that

application of different methodologies can produce different ranking orders with respect to the strength of statistical homogeneity of rock masses. This finding clearly indicates that decision making on statistical homogeneity of rock masses is a difficult task using results coming from just one method. This case study indicates that comparison of results coming from several methods allow one to make better judgement on rock mass statistical homogeneity.

References

Goodman, R.E., 1976. Methods of geological Engineering in discontinuous rocks. West Publishing Co, St Paul, Minn.

Hoek, E., Bray, J.W., 2004. Rock slope Engineering. Taylor & Francis Group, London, and New York, 431p.

Kasatskin, S.A., Golozubov, V.V., Phung, V.P., Le, D.A., 2014. Evidence of Cenozoic Strike-Slip Dislocations of the Red River fault system in Paleozoic Carbonate Strata of Cat Ba Island (northern Vietnam) Russian Journal of Pacific Geology. 8(3), 163-176.

Kulatilake, P.H.S.W., Chen, J., Teng, J., Shufang, X., Pan, G., 1996. Discontinuity geometry characterization for the rock mass around a tunnel close to the permanent ship-lock area of the Three Gorges Dam site in China. Int. J. Rock Mech. and Min. Sci. 33, 255-277.

Kulatilake, P.H.S.W., Fiedler, R., Panda, B.B., 1997. Box fractal dimension as a measure of statistical homogeneity of jointed rock masses. Engineering Geology. 48(3-4), 217-230.

Kulatilake, P.H.S.W., Wathugala, D.N., Poulton, M., Stephansson, O., 1990. Analysis of structural homogeneity of rock masses. Engineering Geology. 29(3), 195-211.

Lancaster, H.O., 1969. The chi-squared distribution. Wiley, New York, 175p.

Li, Y., Wang, Q., Chen, J., Song, S., Ruan, Y., Zhang, Q., 2015. A multivariate technique for evaluating the statistical homogeneity of jointed rock masses. Rock Mechanics and Rock Engineering. 48(5), 1821-1831.

Mahtab, M.A., Yegulalp, T.M., 1984 A similarity test in grouping data in rock mechanics. Proc 25th US Symposium in Rock Mechanics. New York, 495-502.

Martin, M.W., Tannant, D.D., 2004. A technique for identifying structural domain boundaries at the EKATI Diamond Mine. Engineering Geology. 74, 247-264.

Miller, S.M., 1983 A statistical method to evaluate homogeneity of structural populations. Math Geol. 15, 317-328.

Nguyen, T.Y., 1991. Main features of modern geodynamic in the North Vietnam. Geology-Resource, National Centre for Natural Science and Technology Institute of Geology, 7-10. In Vietnamese.

Nguyen, K.Q., Dinh, T.T., Tran, V.T., Dao, D.T., Le, V.C., Nguyen, D.D., Nguyen, T.V., Nguyen, V.H., Pham, V.H., Phan, C.T., Tong, D.T., Tran, T.T., Trinh, D., Vu, K., 2000. Geological and Mineral Resources

Map of Viet Nam on 1:200.000: Backan (F-48-XVI). Department of Geology and Minerals of Vietnam, Hanoi.

Phi, N.Q., Gi, H.S., Thanh, P.T., Phuong, N., 2012. Structural domain identification by fracture orientation and fracture density in rock mass. International Journal of Geoinformatics. 8, 35-40.

Phung, V.P., Nguyen, T.Y., Vu, V.C., 1996. Geodynamic situation in neotectonic and recent period on territory of Vietnam. Geology-Resource, National Centre for Natural Science and Technology institute of geology. I, 101-111. In Vietnamese.

Rocscience, Inc., 2019. Dips v7.0 graphical and statistical analysis of orientation data. Toronto, Ontario, Canada

Song, S., Sun, F., Zhang, W., Chen, J., Xu P., Niu, C., Cao, C., Zhan, J., 2018. Identification of structural domains by considering multiple discontinuity characteristics: a case study of the Songta Dam. Bulletin of Engineering Geology and the Environment. 77(4), 1589-1598.

Thanh, T.P., Gi, H.S., Phi, N.Q., 2015. Delineate structural boundary from fracture correlation coefficients. Vietrock 2015 an ISRM specialized conference, Hanoi, 243-251.

Thanh, P.T., 2019. Tectonic Activity Phases of Cenozoic Period in Xuat Hoa Area, Bac Kan Province, Northeast Region, Vietnam. Indonesian Journal on Geoscience. 6(3), 311-325.

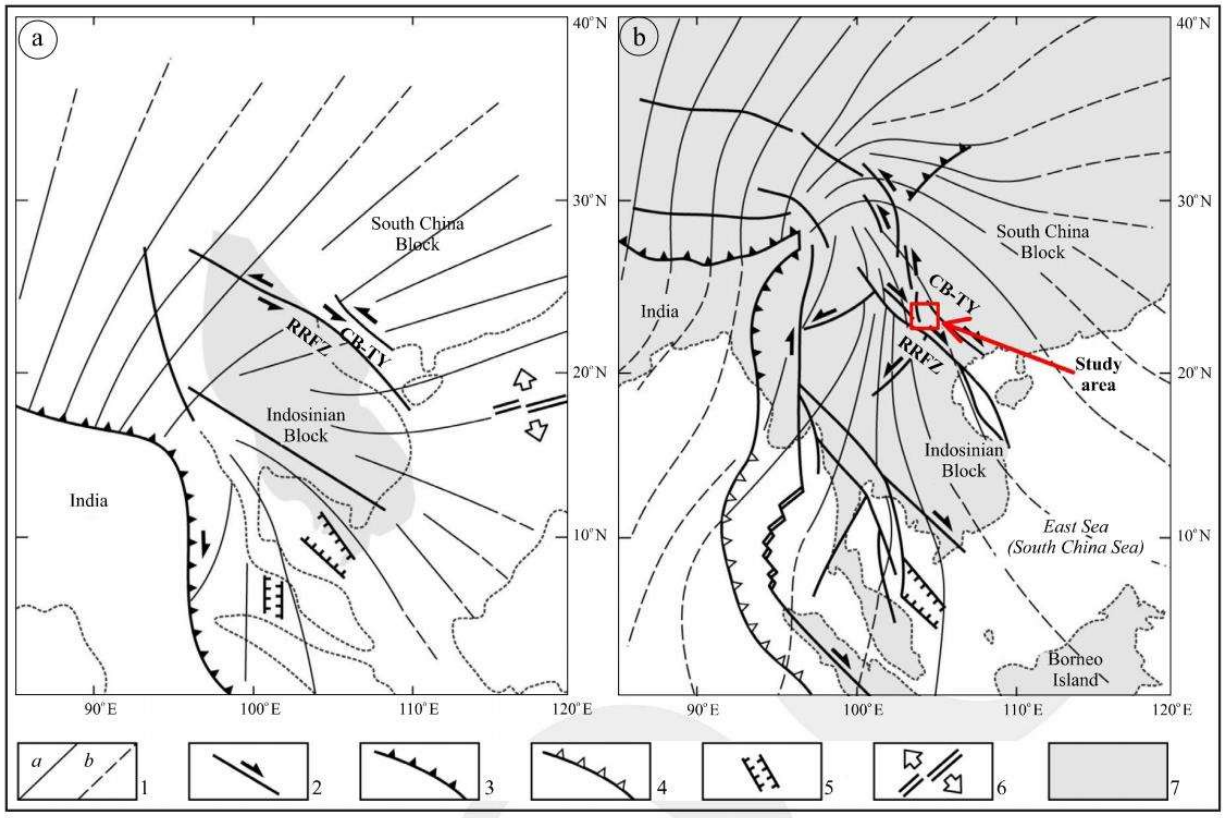

Fig. 1. Trajectories of the maximum compressive stress within the Indochina Peninsula during (a) the Oligocene and (b) at the present time (Kasatkin et al., 2014). The legend on the map in Figure 1 is described as follows: 1. trajectories of the maximum compressive stress: (a) which are directly related to the Indo-Eurasian plate collision and (b) its far-field effects; (2) faults and directions of displacement (arrows); (3) zone of continental collision; (4) subduction zone; (5) extension structures; (6) spreading zones; (7) current position of the land; Red River Fault System (RRFS); Cao Bang - Tien Yen fault (CB - TY).

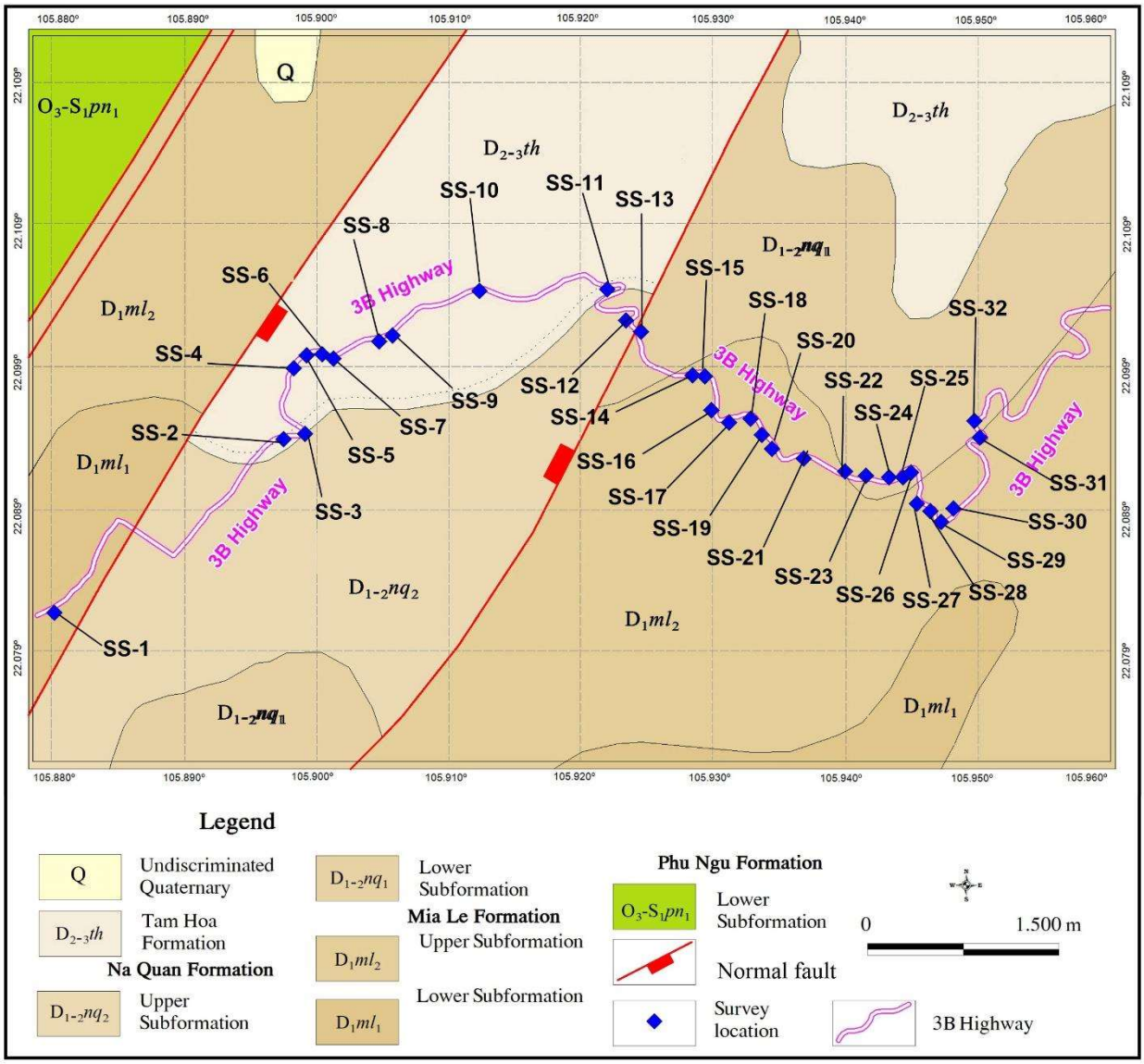

Fig. 2. Geological map of the study area showing the survey stations (SS) used to obtain orientation data.

(a) Tam Hoa ($D_{2\text{-}3}th$) formation at SS-11

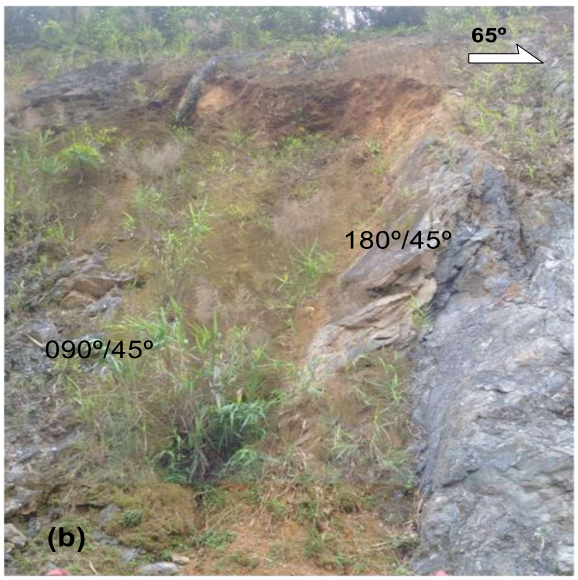

(b) Na Quan Formation ($D_{1\text{-}2nq2}$) at site SS-12

(c) Mia Le Formation (D_1ml_2) at site SS-19

(d) Mia Le Formation (D_1ml_2) at site SS-27

Fig. 3. Typical rock masses that exist at a few survey stations.

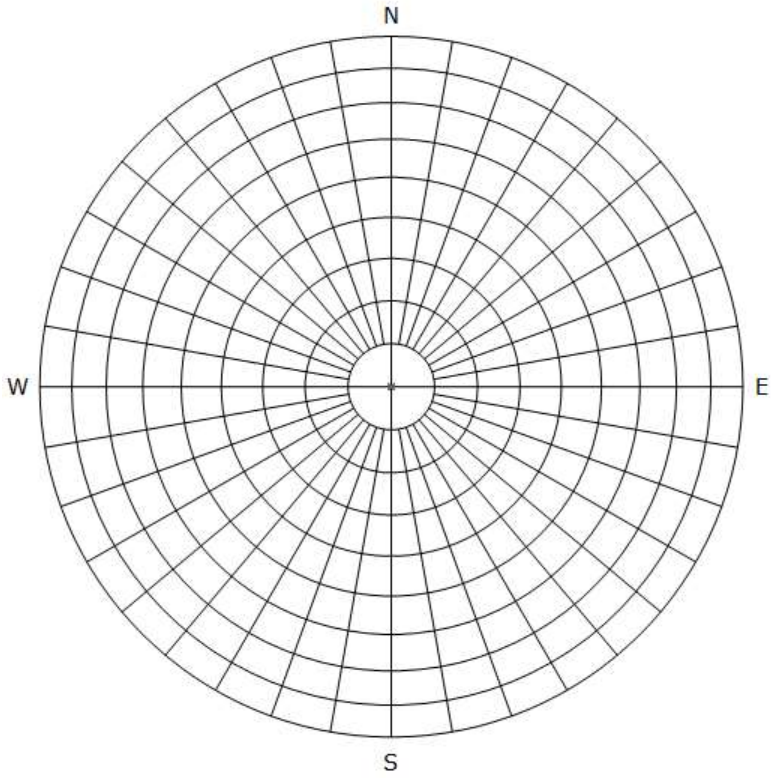

Fig. 4. The constructed 324-patch polar equal area net.

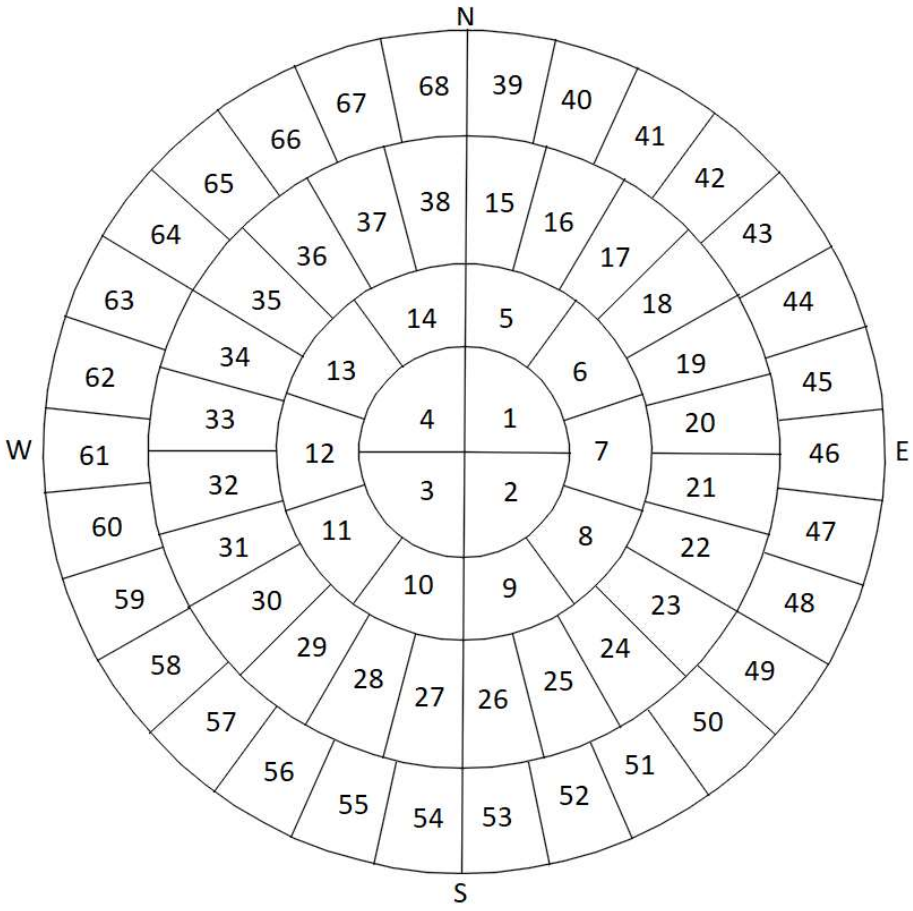

Fig. 5. The designed 68-cell patch network used for the contingency table analysis.

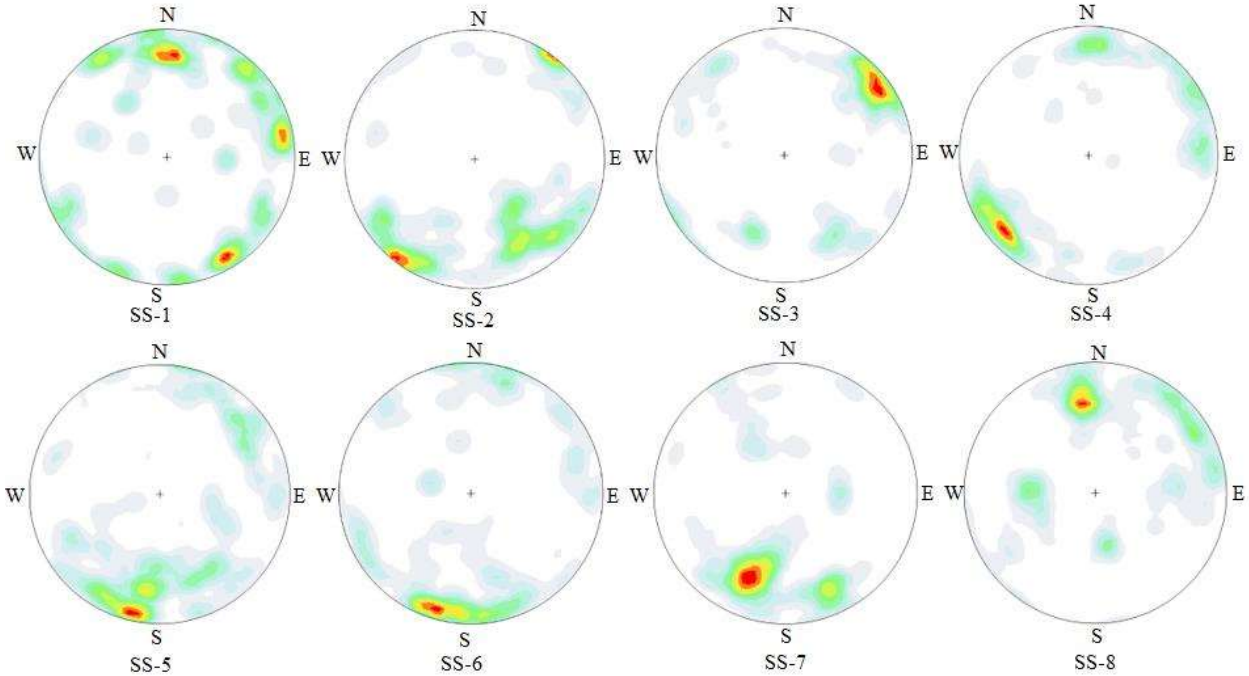

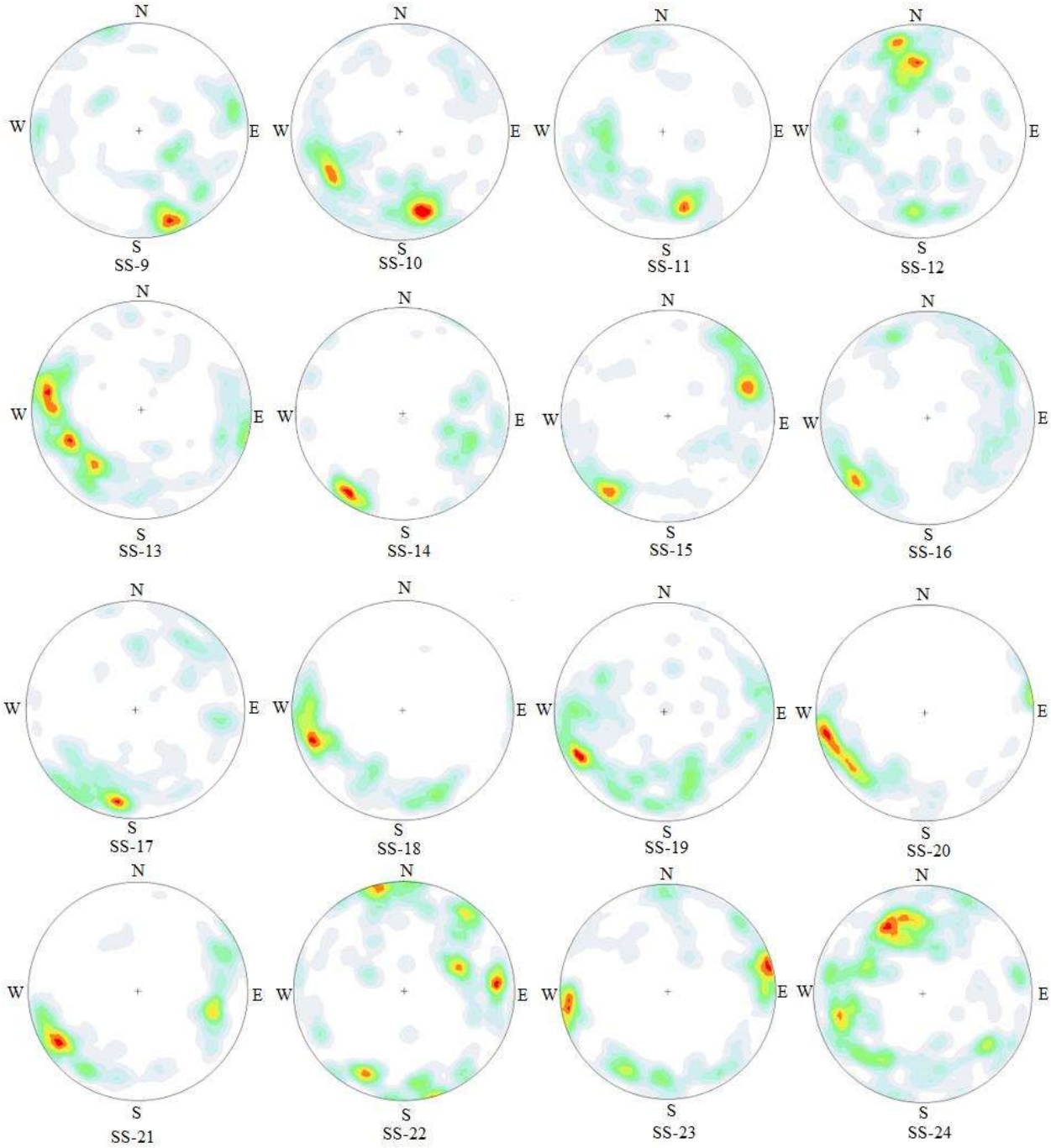
N
W
E
S
SS-9
SS-10
SS-11
SS-12
SS-13
SS-14
SS-15
SS-16
SS-17
SS-18
SS-19
SS-20
SS-21
SS-22
SS-23
SS-24

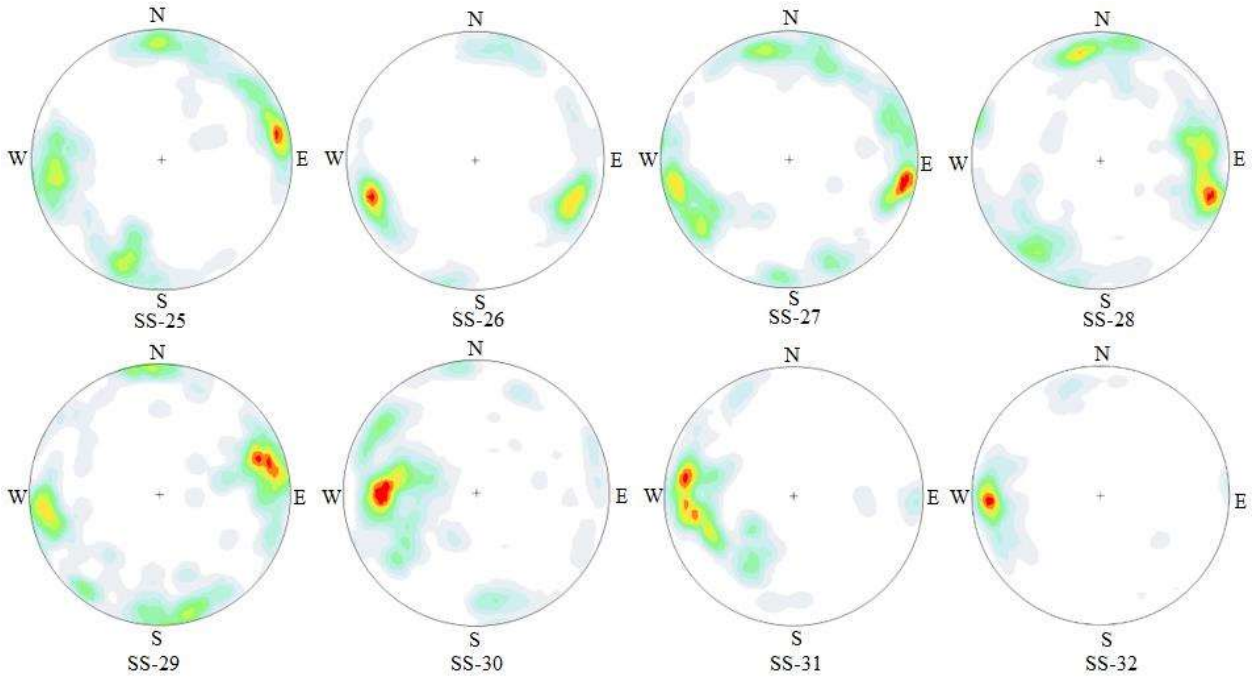

Fig. 6. Lower hemispherical polar equal area pole plots of the 32 stations located along the highway corridor.

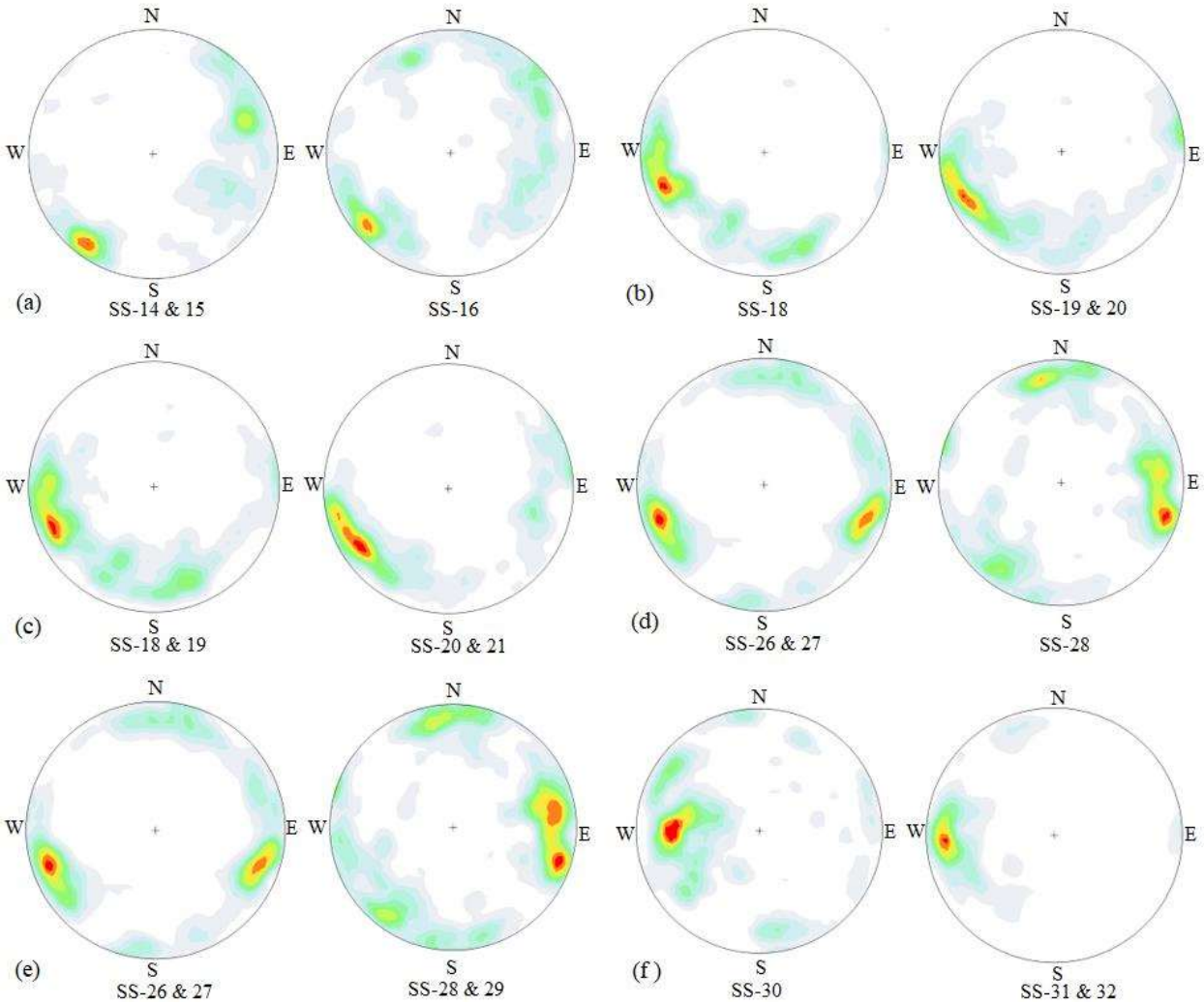

Fig. 7. Lower hemispherical polar equal area pole plot comparisons made for the combined stations: (a) SS-14 & 15 versus SS-16 (L level), (b) SS-18 versus SS-19 & 20 (H level), (c) SS-18 & 19 versus SS-20 & 21 (M level), (d) SS-26 & 27 versus SS-28 (L level), (e) SS-26 & 27 versus SS-28 & 29 (L level) and (f) SS-30 versus SS-31 & 32 (L level).

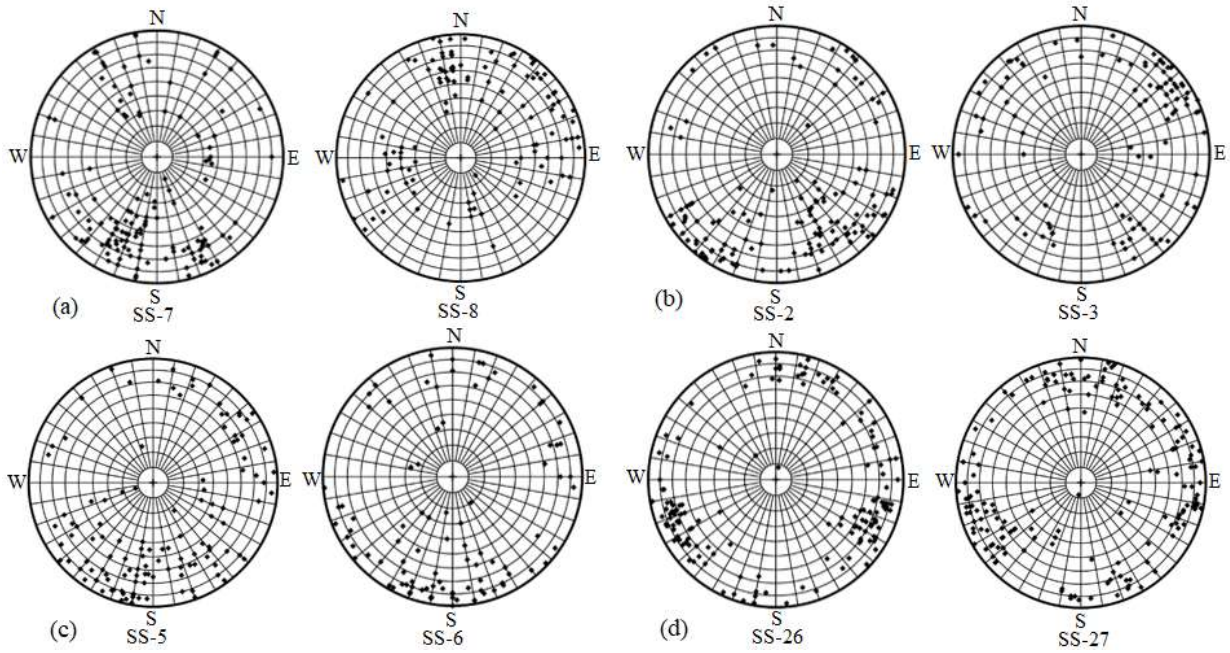

Fig. 8. Pole plot comparisons on the 324-patch network for R analysis as typical examples for poor, low, moderate, and high R values: (a) SS-7 versus SS-8 (poor R = -0.04), (b) SS-2 versus SS-3 (low R = 0.24), (c) SS-5 versus SS-6 (moderate R = 0.38) and (d) SS-26 versus SS-27 (high R = 0.58).

Table 1 Survey station locations, geologic age and the number of discontinuity orientation data collected for the various stations.

Survey station number	Longitude	Latitude	Geological age	Number of discontinuities
SS-1	105°52’56.8”	22°04’46.5”	D_1ml_1	73
SS-2	105°53’52,2”	22°5’37,6”;	$D_{2-3}th$	127
SS-3	105°53’53.7”	22°05’09.2”	$D_{2-3}th$	103
SS-4	105°53’56.2”	22°05’55.8”	$D_{2-3}th$	116
SS-5	105°53’59.8”	22°05’59.1”	$D_{2-3}th$	122
SS-6	105°54’03.9”	22°05’59.4”	$D_{2-3}th$	96
SS-7	105°54’07.0”	22°05’58.2”	$D_{2-3}th$	137
SS-8	105°54’19.5”	22°06’02.5”	$D_{2-3}th$	119
SS-9	105°54’23.1”	22°06’03.9”	$D_{2-3}th$	105
SS-10	105°54’46.9”	22°06’15.1”	$D_{2-3}th$	188
SS-11	105°52’21,8”	22°06’15.6”	$D_{2-3}th$	136
SS-12	105°55’28.2”	22°06’09.3”	$D_{1-2}nq_2$	113
SS-13	105°55’30.8”	22°06’04.6”	$D_{1-2}nq_2$	135
SS-14	105°55’44.7”	22°05’53.4”	D_1ml_2	71
SS-15	105°55’48.1”	22°05’53.1”	D_1ml_2	167
SS-16	105°55’49.8”	22°05’44.6”	D_1ml_2	165
SS-17	105°55’54.6”	22°05’41.4”	D_1ml_2	141
SS-18	105°56’00.5”	22°05’42.3”	D_1ml_2	104
SS-19	105°56’03.5”	22°05’38.2”	D_1ml_2	120
SS-20	105°56’06.2”	22°05’34.7”	D_1ml_2	103
SS-21	105°56’14.8”	22°05’32.1”	D_1ml_2	119
SS-22	105°56’26.0”	22°05’28.8”	$D_{1-2}nq_1$	99
SS-23	105°56’31.8”	22°05’27.7”	$D_{1-2}nq_1$	128
SS-24	105°56’38.1”	22°05’27.2”	$D_{1-2}nq_1$	152
SS-25	105°56’41.8”	22°05’27.3”	$D_{1-2}nq_1$	155
SS-26	105°56’44.1”	22°05’24.7”	$D_{1-2}nq_1$	158
SS-27	105°56’45.6”	22°05’20.6”	D_1ml_2	172
SS-28	105°56’49.2”	22°05’18.6”	D_1ml_2	215
SS-29	105°56’52.1”	22°05’15.9”	D_1ml_2	102
SS-30	105°56'55.5"	22°05'19.3"	D_1ml_2	205
SS-31	105°57'02.8"	22°05'37.2"	D_1ml_2	103
SS-32	105°57'01.3"	22°05'41.4"	$D_{1-2}nq_1$	140

Table 2 Contingency table for analyzing the polar equal area plots of different stations (after Miller, 1983).

Columns				
Rows	Patch 1	Patch 2	Patch 3	Row totals
Equal area plot 1	f_{11}	f_{12}	f_{1c}	R_1
Equal area plot 2	f_{21}	f_{22}	f_{21}	R_2
.	-	-	-	-
.	-	-	-	-
.	-	-	-	-
Equal area plot r	f_{r1}	f_{r2}	f_{rc}	R_r
Column totals	C_1	C_2	C_c	N

f_{ij}= number of discontinuity poles observed in cell ij ; N = total number of discontinuity poles from all equal area plots.

Table 3 Summary results for strength of statistical homogeneity based on different methods.

Tested combinations	Avg. max. sig. value based on normal dist.	Avg. max. sig. value based on chi- square dist.	Avg. max. sig. value based on chi- square and normal dists.	Rank based on contingency table analysis results	Rank based on R value	R value	Qualitative rank based on equal area and pole plot comparisons
SS1-SS2	0.0216	0.0351	0.0283	18	23	0.18	P
SS2-SS3	0.003	0.0112	0.0071	23	16	0.24	L-P
SS3-SS4	0.0007	0.0054	0.0062	24	21	0.21	L-P
SS4-SS5	0.1711	0.1222	0.1467	14	20	0.22	L
SS5-SS6	0.3214	0.184	0.2527	7	9	0.38	M
SS6-SS7	0.1199	0.0921	0.106	17	22	0.20	L
SS7-SS8	0	0	0	31	31	-0.04	P
SS8-SS9	0	0.0002	0.0001	30	29	0.08	P
SS9-SS10	0.0078	0.0156	0.0117	20	14	0.25	L-P
SS10-SS11	0.5002	0.2708	0.3855	3	5	0.47	M
SS11-SS12	0.1508	0.114	0.1324	16	16	0.24	L
SS12-SS13	0.005	0.0131	0.0091	22	30	0.04	P
SS13-SS 14	0	0.0008	0.0004	27	28	0.11	P
SS14-SS15	0.2076	0.1365	0.1721	10	8	0.41	M
SS15-SS16	0.1965	0.14	0.1683	11	12	0.33	M
SS16-SS17	0.2172	0.1383	0.1778	9	16	0.24	L
SS17-SS18	0	0.0003	0.0002	29	27	0.15	P
SS18-SS19	0.1909	0.1353	0.1631	12	10	0.37	M
SS19-SS20	0.4857	0.2701	0.3779	4	6	0.45	M
SS20-SS21	0.5792	0.5048	0.542	2	3	0.50	H
SS21-SS22	0.0046	0.0168	0.0107	21	23	0.18	P
SS22-SS23	0.1959	0.1214	0.1586	13	19	0.23	L
SS23-SS24	0.0182	0.0088	0.0135	19	23	0.18	P
SS24-SS25	0	0.0005	0.0003	28	14	0.25	P
SS25-SS26	0	0.001	0.0005	26	13	0.32	L-P
SS26-SS27	0.8679	0.4426	0.6553	1	1	0.58	H
SS27-SS28	0.4129	0.2343	0.3236	5	4	0.48	H
SS28-SS29	0.1607	0.1117	0.1362	15	11	0.35	M
SS29-SS30	0.0002	0.002	0.0011	25	26	0.16	P
SS30-SS31	0.2147	0.1428	0.1788	8	7	0.43	M
SS31-SS32	0.3998	0.2297	0.3148	6	2	0.56	H
SS14&15-SS16	0.0526	0.0601	0.0564	17-18	13-14	0.30	L
SS18-SS19&20	0.5658	0.3348	0.4503	2-3	1-2	0.57	H
SS18&19-SS20&21	0.0517	0.0527	0.0522	17-18	1-2	0.57	M
SS26&27-SS28	0.0036	0.0095	0.0066	23-24	3	0.50	L
SS26&27-SS28&29	0.001	0.0051	0.0031	24-25	2-3	0.55	L
SS30-SS31&32	0.0006	0.0096	0.0051	24-25	9	0.38	L

Conflict of interest/competing interest

The authors declare that they have no conflict of interest.